

Magnetism and Correlations in Fractionally Filled Degenerate Shells of Graphene Quantum Dots

A. D. Güçlü,¹ P. Potasz,^{1,2} O. Voznyy,¹ M. Korkusinski,¹ and P. Hawrylak¹

¹*Institute for Microstructural Sciences, National Research Council of Canada, Ottawa, Canada*

²*Institute of Physics, Wrocław University of Technology, Wrocław, Poland*

(Received 11 August 2009; published 10 December 2009)

We show that the ground state and magnetization of the macroscopically degenerate shell of electronic states in triangular gated graphene quantum dots depends on the filling fraction of the shell. The effect of degeneracy, finite size, and electron-electron interactions are treated nonperturbatively using a combination of density functional theory, tight-binding, Hartree-Fock and configuration interaction methods. We show that electronic correlations play a crucial role in determining the nature of the ground state as a function of filling fraction of the degenerate shell at the Fermi level. We find that the half-filled charge neutral shell leads to full spin polarization but this magnetic moment can be completely destroyed by adding a single electron.

DOI: [10.1103/PhysRevLett.103.246805](https://doi.org/10.1103/PhysRevLett.103.246805)

PACS numbers: 73.63.Kv, 73.23.Hk, 73.43.Lp, 75.75.+a

Following the progress in the fabrication of graphene [1–5] based devices, lower dimensional structures such as graphene ribbons [6–9], and more recently graphene quantum dots [10–14], are attracting increasing attention due to their nontrivial electronic and magnetic properties. In particular, it was shown that when an electron is confined to a triangular atomic thick layer of graphene with zigzag edges, its energy spectrum collapses to a shell of degenerate states at the Fermi level (Dirac point) [15–19] similar to the edge states in graphene ribbons [6–9], but isolated from remaining states by a gap. The degeneracy is proportional to the edge size and can be made macroscopic. This opens up the possibility to design a strongly correlated electronic system as a function of fractional filling of the shell, in analogy to the fractional quantum Hall effect [20], but without the need for a magnetic field.

In this work we present new results demonstrating the important role of electronic correlations beyond the Hubbard model [15–17] and mean-field density functional theory (DFT) [17,18]. The interactions are treated by a combination of DFT, tight-binding (TB), Hartree-Fock (HF) and configuration interaction (CI) methods. We show that a half-filled charge neutral shell leads to full spin polarization of the island but this magnetic moment is completely destroyed by the addition of a single electron, in analogy to the effect of Skyrmions on the quantum Hall ferromagnet [21–24] and spin depolarization in electrostatically defined semiconductor quantum dots [25–28]. The depolarization of the ground state is predicted to result in blocking of current through a graphene quantum dot due to the spin blockade (SB) in single electron transport [26,28]: the transition between maximally polarized and depolarized ground states cannot be accomplished by the addition of a spin of a single electron.

Figure 1(a) shows the electronic density of a zigzag edged triangular island of $N = 97$ carbon atoms, separated by a distance d_{gate} from a metallic gate. At zero applied

voltage the island is charge neutral while applied voltage leads to removal or addition of electrons to the island. The single-particle energy spectrum obtained using nearest neighbor tight-binding method (TB, blue lines) and a combination of the next-nearest neighbor tight-binding and Hartree-Fock methods (TB + HF, black lines) is shown in Fig. 1(b). As was previously shown by Ezawa [16], Fernandez-Rossier and Palacios [17], and Wang, Meng and Kaxiras [18] using the nearest-neighbor TB method and *ab initio* DFT calculations, the linear spectrum of Dirac electrons in bulk graphene collapses to a shell of degenerate levels at the Fermi energy, well separated in energy from the valence and conduction bands. Similar to edge states in graphene ribbons [6–9], the zigzag edge breaks the symmetry between the two sublattices of the honeycomb lattice, behaving like a defect. Therefore, electronic states localized on the zigzag edges appear with energy in the vicinity of the Fermi level. For a $N = 97$ atoms island (see Fig. 1) there are $N_{\text{edge}} = 7$ edge states. For the charge neutral system there is one electron per each edge state. A nontrivial question addressed here is the specific spin and orbital configuration of the electrons as a function of the size and the fractional filling of the degenerate shell of edge states. Because of the strong degeneracy, many-body effects can be expected to be important as in the fractional quantum Hall effect. Previous calculations based on the Hubbard approximation [15–17] and local spin density functional theory [17,18] showed that the neutral system (half-filling) has its edge states polarized.

In order to study many-body effects within the charged degenerate shell via the configuration interaction method, we first perform a Hartree-Fock calculation for the charged system of $N - N_{\text{edge}}$ electrons, with empty degenerate shell and N_{edge} electrons transferred to the gate, shown in Fig. 1(a) [29]. The spectrum of HF quasiparticles is shown with black lines in Fig. 1(b). Because of the mean-field

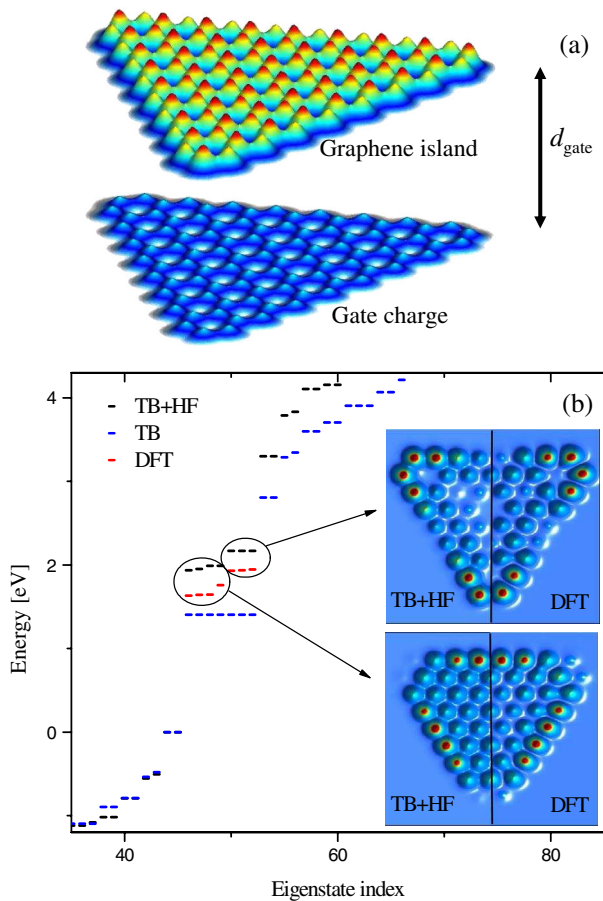


FIG. 1 (color online). (a) Electronic density in a triangular graphene island of 97 carbon atoms where 7 electrons were moved to the metallic gate at a distance of d_{gate} . (b) Single-particle spectrum of the structure in (a), obtained by tight-binding (TB, blue lines) and self-consistent Hartree-Fock (TB + HF, black lines) methods. The 7 zero-energy states near the Fermi level are compared to DFT results. In Hartree-Fock and DFT calculations 7 electrons were removed, leaving the zero-energy states empty. The dielectric constant κ is set to 6. Inset compares the structure of corner and side states obtained using Hartree-Fock and DFT calculations. In DFT calculations, hydrogen atoms were attached to dangling bonds.

interaction with the valence electrons and charged gate, a group of three states is now separated from the rest by a small gap of ~ 0.2 eV. The three states correspond to HF quasiparticles localized in the three corners of the triangle. The same physics occurs in density functional calculation within local density approximation (LDA), shown with red lines in Fig. 1(b). Hence we see that the shell of almost degenerate states with a well defined gap separating them from the valence and conduction bands exists in the three approaches.

The wave functions corresponding to the shell of nearly-degenerate zero-energy states obtained from TB-HF calculations are used as a basis set in our configuration interaction calculations where we add N_{add} electrons

from the gate to the shell of degenerate states. In Fig. 2, total spin S of the ground state as a function of the filling of the degenerate shell is shown for different sizes of quantum dots. Three aspects of these results are particularly interesting. (i) For the charge neutral case ($N_{\text{add}} - N_{\text{edge}} = 0$), for all the island sizes studied ($N_{\text{edge}} = 3-7$), the half-filled shell is maximally spin polarized as indicated by red (light gray) arrows, in agreement with our DFT calculations which reproduce previous work [17,18]. The polarization of the half-filled shell is also consistent with the Lieb theorem for the Hubbard model for a bipartite lattice [30]. (ii) The spin polarization is fragile. If we add one extra electron ($N_{\text{add}} - N_{\text{edge}} = 1$), magnetization of the island collapses to the minimum possible value, as indicated by blue (dark gray) arrows in Fig. 2. Full or partial depolarization occurs for other filling numbers. (iii) The spin phase diagram is not necessarily symmetric around $N_{\text{add}} - N_{\text{edge}} = 0$. The main reason for the broken electron-hole symmetry is the imbalance between the two types of atoms of the honeycomb lattice in the triangular

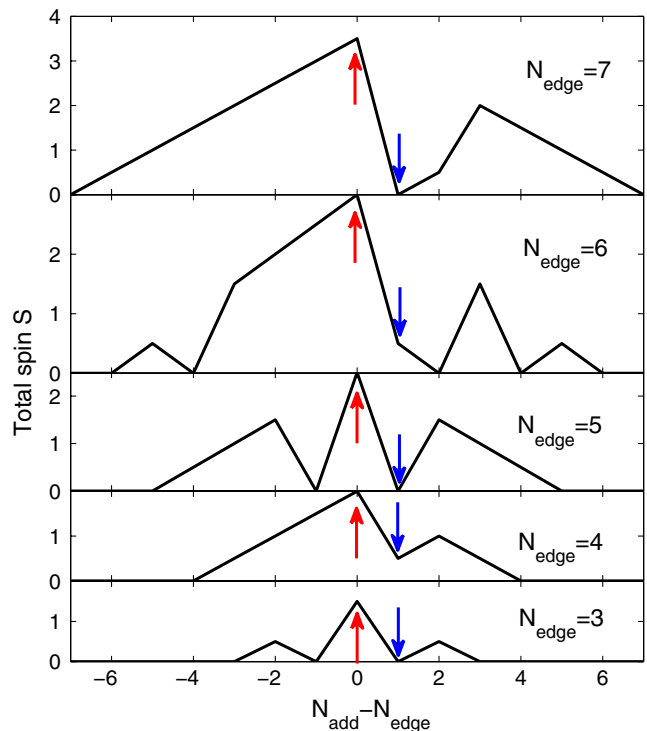


FIG. 2 (color online). Spin phase diagram from the TB-HF-CI method for different sizes of the triangular dot characterized by the number of edge states N_{edge} , as a function of the filling of the zero-energy states $N_{\text{add}} - N_{\text{edge}} = 0$. Charge neutral case corresponds to $N_{\text{add}} - N_{\text{edge}} = 0$, for which the total spin of the zero-energy electrons are always maximized ($S = N_{\text{edge}}/2$, indicated by red [light gray] arrows). On the other hand, if the quantum dot is charged by 1 electron ($N_{\text{add}} - N_{\text{edge}} = 1$) then the total spin has minimum value, i.e. $S = 0$ if N_{add} is even, $S = 1/2$ if N_{add} is odd (indicated by blue [dark gray] arrows).

zigzag structure (the next-nearest neighbor hopping also contributes to the breaking of the symmetry). The broken electron-hole symmetry can be seen from Fig. 1 where the corner states are separated from the rest of the zero-energy states by a small gap. As a result, there is a delicate competition between total kinetic energy and the interaction energy as a function of the size of the triangle and the number of electrons, causing the nonsymmetric behavior of the spin phase diagram for $N_{\text{edge}} = 4, 6$ and 7 . Finally, the spin depolarization at half-filling was found to be insensitive to the screening of electron-electron interactions, as values of dielectric screening constant κ between 2 and 8 led to the same behavior of the charge neutral and single electron charged cases (not shown).

In order to illuminate the depolarization process as an electron is added to the charge neutral maximally spin polarized system, in Figs. 3(a) and 3(b) we show the orbital occupancy of up-spin zero-energy states at $N_{\text{add}} - N_{\text{edge}} = 1$, for the fully polarized state $S = 3$ (upper panel) and for the ground state, $S = 0$, (lower panel) for the $N_{\text{site}} = 97$ atoms quantum dot with 7 zero-energy states shown in Fig. 1. For the large spin $S = 3$ case, the added spin-up electron simply occupies the orbital 1 and its spin is opposite to the spins of the other 7 electrons. However, the true ground state has $S = 0$, with the spin occupancy shown in the lower panel. The added electron causes electrons already present to partially flip their spin, with spin-up density being delocalized over all the 7 orbitals in analogy to Skyrmin-like excitations in quantum dots and quantum Hall ferromagnets [21–24]. The correlated nature of the $S = 0$ spin depolarized ground state is illustrated by the up-up spin pair correlation functions given by $\langle \rho_{\uparrow}(\mathbf{r}_0)\rho_{\uparrow}(\mathbf{r}) \rangle$, shown in Figs. 3(c) and 3(d). The location of the fixed up-spin electron at site \mathbf{r}_0 is schematically shown with an up arrow. The up-up spin correlation function for the $S = 3$ spin polarized system is strictly zero as

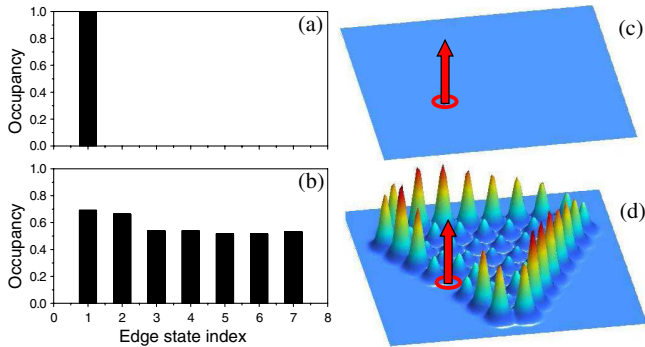


FIG. 3 (color online). Left panel: Orbital occupancy of the 7 zero-energy states by spin-up electrons, for the charged ($N_{\text{add}} - N_{\text{edge}} = 1$) system, for (a) $S = 3$ and (b) $S = 0$ total spin states. The ground state is $S = 0$ (see Fig. 2). Right panel: Corresponding spin up-up pair-correlation functions $\langle \rho_{\uparrow}(\mathbf{r}_0)\rho_{\uparrow}(\mathbf{r}) \rangle$. The fixed spin-up electron is represented by a red arrow, and its position \mathbf{r}_0 by a red circle.

there are no other spin-up electrons. The spin correlation function for the spin depolarized ground state with $S = 0$ shows the exchange hole at \mathbf{r}_0 , which extends to the nearest neighbors, and, more interestingly, for larger $|\mathbf{r}_0 - \mathbf{r}|$, the spin pair correlation function reveals a spin texture: Beyond the exchange hole there is the formation of an electronic cloud with positive magnetization which decreases and changes sign at even larger distance, again consistent with the Skyrmin picture [21,22].

Experimentally, spin properties of quantum dots can be probed using Coulomb and spin blockade spectroscopy [28]. By connecting graphene quantum dot to leads and measuring the conductance as a function of gate voltage, one obtains a series of Coulomb blockade peaks. The relative position of these peaks and their height reveal information about the electronic properties of the system as the number of electrons is increased. The amplitude of

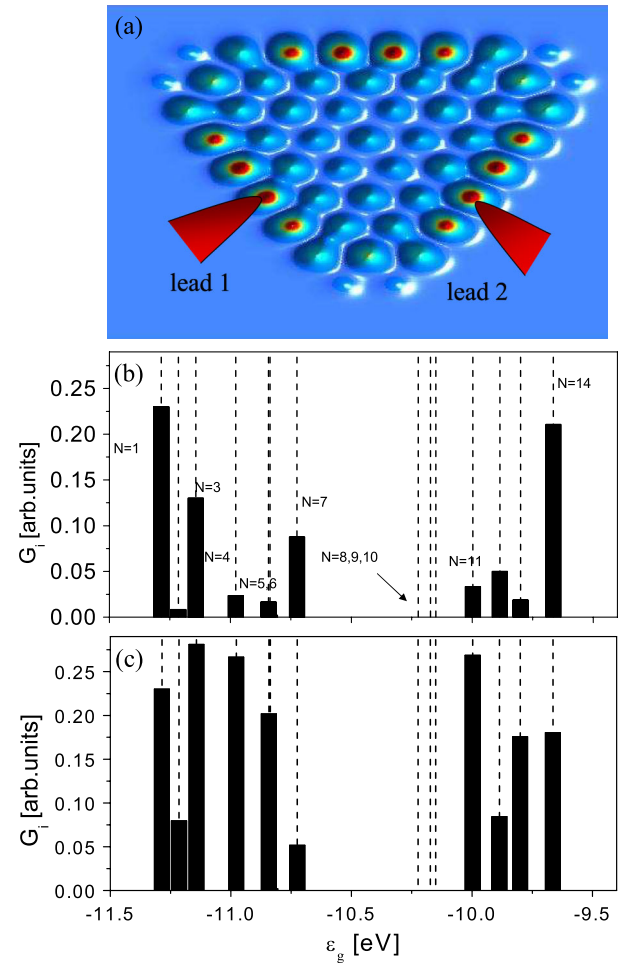


FIG. 4 (color online). (a) Schematic representation of the graphene island connected to the leads through a side site. (b) Conductivity as a function of the shift in single-particle energies due to applied gate voltage, ϵ_g , (c) Same as (b) but without the site dependence of the incoming electron. The oscillations of the spectral weight in (c) are purely due to correlation effects and spin blockade.

the Coulomb blockade peak is given by the conductivity G_i of the graphene quantum dot connected to leads via atom “ i ” [31] as shown schematically in Fig. 4(a). Spin and correlation effects are reflected in the weight of the Coulomb blockade peak proportional to the matrix element $|\langle N+1, J', S' | c_{i\sigma}^\dagger | N, J, S \rangle|^2$ which gives the transition probability from state (N, J, S) to state $(N+1, J', S')$ when an additional electron is added to the site “ i ” of the graphene quantum dot from the lead [29]. The ground state configuration (N, J, S) is controlled by the gate voltage. For our model graphene quantum dot with 7 degenerate zero-energy states, we can add a total of 14 electrons. Hence, one expects to obtain 14 Coulomb blockade peaks. In Fig. 4(b) some of the peaks have zero height due to the spin blockade phenomenon. For instance, the transitions from $(N=7, S=7/2)$ states to $(N=8, S=0)$ states are spin blocked since it is not possible to change the spin of the system by $\Delta S = -7/2$ by adding one electron with $S=1/2$. Similarly, transitions from $(N=9, S=1/2)$ states to $(N=10, S=4/2)$ states are spin blocked. Besides the spin blockade, one sees strong oscillations of the spectral function heights. This is due to (a) strongly correlated nature of the states $|N, S\rangle$, and (b) specific choice of the site “ i ,” where the lead is attached to. Here, we chose a site close to the middle of one of the sides of the triangle. The overlap of the site wave function is strongly dependent on the nature of the zero-energy states. In particular, the existence of corner states, as discussed in Fig. 1, strongly affects the transition probabilities. To isolate the effect of correlation to the lead’s position, in Fig. 4(c) we plot the conductivity assuming that the weight of the site “ i ” is a constant independent of the zero-energy state. As a result, the weights of spectral peaks are different, except for $N=8, 9, 10$ where the spin blockade occurs. These results show how to detect the spin depolarization in transport experiments. Ultimately, we show here that one can design a strongly correlated electron system in carbon based material whose magnetic properties can be controlled by applied gate voltage.

The authors thank NRC-CNRS CRP, Canadian Institute for Advanced Research, Institute for Microstructural Sciences, and QuantumWorks for support.

-
- [1] K. S. Novoselov, A. K. Geim, S. V. Morozov, D. Jiang, Y. Zhang, S. V. Dubonos, I. V. Grigorieva, and A. A. Firsov, *Science* **306**, 666 (2004).
 [2] K. S. Novoselov, A. K. Geim, S. V. Morozov, D. Jiang, M. I. Katsnelson, I. V. Grigorieva, S. V. Dubonos, and A. A. Firsov, *Nature (London)* **438**, 197 (2005).
 [3] Y. B. Zhang, Y. W. Tan, H. L. Stormer, and P. Kim, *Nature (London)* **438**, 201 (2005).

- [4] S. Y. Zhou, G. H. Gweon, J. Graf, A. V. Fedorov, C. D. Spataru, R. D. Diehl, Y. Kopelevich, D. H. Lee, S. G. Louie, and A. Lanzara, *Nature Phys.* **2**, 595 (2006).
 [5] A. H. C. Neto, F. Guinea, N. M. R. Peres, K. S. Novoselov, and A. K. Geim, *Rev. Mod. Phys.* **81**, 109 (2009).
 [6] K. Nakada, M. Fujita, G. Dresselhaus, and M. S. Dresselhaus, *Phys. Rev. B* **54**, 17954 (1996).
 [7] K. Wakabayashi, M. Fujita, H. Ajiki, and M. Sigrist, *Phys. Rev. B* **59**, 8271 (1999).
 [8] B. Wunsch, T. Stauber, F. Sols, and F. Guinea, *Phys. Rev. Lett.* **101**, 036803 (2008).
 [9] L. Yang, M. L. Cohen, and S. G. Louie, *Phys. Rev. Lett.* **101**, 186401 (2008).
 [10] B. Wunsch, T. Stauber, and F. Guinea, *Phys. Rev. B* **77**, 035316 (2008).
 [11] J. Wurm, A. Rycerz, I. Adagideli, M. Wimmer, K. Richter, and H. U. Baranger, *Phys. Rev. Lett.* **102**, 056806 (2009).
 [12] A. R. Akhmerov and C. W. J. Beenakker, *Phys. Rev. B* **77**, 085423 (2008).
 [13] F. Libisch, C. Stampfer, and J. Burgdorfer, *Phys. Rev. B* **79**, 115423 (2009).
 [14] Z. Z. Zhang, K. Chang, and F. M. Peeters, *Phys. Rev. B* **77**, 235411 (2008).
 [15] M. Ezawa, *Phys. Rev. B* **76**, 245415 (2007).
 [16] M. Ezawa, *Phys. Rev. B* **77**, 155411 (2008).
 [17] J. Fernandez-Rossier and J. J. Palacios, *Phys. Rev. Lett.* **99**, 177204 (2007).
 [18] W. L. Wang, S. Meng, and E. Kaxiras, *Nano Lett.* **8**, 241 (2008).
 [19] J. Akola, H. P. Heiskanen, and M. Manninen, *Phys. Rev. B* **77**, 193410 (2008).
 [20] D. C. Tsui, H. L. Stormer, and A. C. Gossard, *Phys. Rev. Lett.* **48**, 1559 (1982).
 [21] S. L. Sondhi, A. Karlhede, S. A. Kivelson, and E. H. Rezayi, *Phys. Rev. B* **47**, 16419 (1993).
 [22] A. H. MacDonald, H. A. Fertig, and L. Brey, *Phys. Rev. Lett.* **76**, 2153 (1996).
 [23] K. Nomura and A. H. MacDonald, *Phys. Rev. Lett.* **96**, 256602 (2006).
 [24] P. Plochocka, J. M. Schneider, D. K. Maude, M. Potemski, M. Rappaport, V. Umansky, I. Bar-Joseph, J. G. Groshaus, Y. Gallais, and A. Pinczuk, *Phys. Rev. Lett.* **102**, 126806 (2009).
 [25] P. Hawrylak, *Phys. Rev. Lett.* **71**, 3347 (1993).
 [26] J. J. Palacios, L. Martín-Moreno, G. Chiappe, E. Louis, and C. Tejedor, *Phys. Rev. B* **50**, 5760 (1994).
 [27] M. Korkusinski, P. Hawrylak, M. Ciorga, M. Piore-Ladriere, and A. S. Sachrajda, *Phys. Rev. Lett.* **93**, 206806 (2004).
 [28] M. Ciorga, A. S. Sachrajda, P. Hawrylak, C. Gould, P. Zawadzki, S. Jullian, Y. Feng, and Z. Wasilewski, *Phys. Rev. B* **61**, R16315 (2000).
 [29] See EPAPS Document No. E-PRLTAO-104-006001 for technical details of the methods. For more information on EPAPS, see <http://www.aip.org/pubservs/epaps.html>.
 [30] E. H. Lieb, *Phys. Rev. Lett.* **62**, 1201 (1989).
 [31] A. D. Güçlü, Q. F. Sun, H. Guo, and R. Harris, *Phys. Rev. B* **66**, 195327 (2002).